Journal of the Oceanographical Society of Japan
Vol. 38, pp. 125 to 130, 1982

Numerical Experiment on the Circulation in the Japan Sea
Part III. Mechanism of the Nearshore Branch of the Tsushima Current*

Jong-Hwan YOON**

Abstract: By using a two-dimensional barotropic model on a β-plane, the effect of the bottom topography on the path of the Tsushima Current is investigated. The rectangular model ocean with continental slopes has two openings: one is located at the southern boundary and the other at the eastern boundary. In a steady state, most of the water supplied into the model ocean through the inflow opening, flows along the continental slope with the coast to the right. Continental shelf waves play an important role in the process of adjustment to a steady state. It is suggested that the nearshore branch of the Tsushima Current might be largely topographically controlled.

1. Introduction

The experiments reported in previous papers of the present study (Part I and II: YOON, 1982, 1982a) did not reproduce the nearshore branch of the Tsushima Current along the Japanese coast. Although a density-driven boundary current appeared along the Japanese coast from summer to autumn in Experiment III in Part II (YOON, 1982a), it was concluded that characteristics of the nearshore branch of the Tsushima Current can not be explained by the density-driven boundary current alone. Bottom topography was ignored in these experiments. The continental shelf and slope might be very important in controlling the flow path because the flow over the bottom topography tends to follow the isobaths of bottom topography to conserve potential vorticity in a steady state. The water supplied throgh the Tsushima Strait might be strongly controlled by this mechanism and, as a result, the water would flow along the Japanese coast over the continental shelf and slope as the nearshore branch of the Tsushima Current. The purpose of this study is to investigate how the current flowing into the Japan Sea is controlled by the continental shelf and slope by using a simple two-dimensional barotropic model.

* Received Aug. 7, 1981; revised Mar. 10 and accepted Mar. 23, 1982.

** Geophysical Institute, Faculty of Science, University of Tokyo, Bunkyô-ku, Tokyo 113, Japan

2. Model

Figure 1 shows a schematic view of the model ocean basin whose dimensions are almost the same as the model ocean basin in Part I (YOON, 1982) except for the bottom topography. The latitudinal and longitudinal lengths are both 900 km. The ocean has two openings; one (inflow opening) is located at the southern wall and the other (outflow opening) at the eastern wall. The width of the inflow and outflow openings are 180 km and 45 km respectively. The depth and the width of the continental shelf along lateral boundaries are 150 m and 22.5 km respectively. The width of the continental slope region is 135 km. The depth of the deepest part of the model ocean is 2,000 m.

Now, let us use a rectangular coordinate

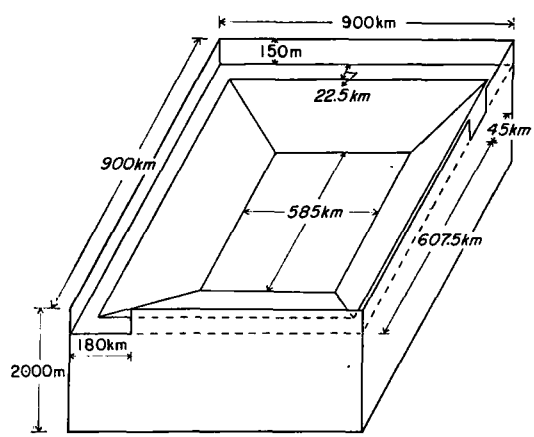

Fig. 1. Schematic view of the model ocean.

system on a β-plane and take x eastward, y northward and z upward from the mean sea surface level. We assume that the ocean is homogeneous and stress free at the bottom and that hydrostatic balance holds. Let u and v be the components of velocity in the x and y directions, h the depth of ocean, A_h the horizontal kinematic eddy viscosity and $f=f_0+\beta y$ ($\beta=2\times10^{-13}\,\mathrm{cm^{-1}\,s^{-1}}$, $f_0=0.9\times10^{-4}\,\mathrm{s^{-1}}$) the Coriolis parameter, respectively. We are interested in the phenomena having a frequency much less than f (the Coriolis parameter), and a horizontal scale less than the Rossby's deformation radius $\sqrt{gh}/f$ ($\sim$1,400 km with $h\sim$2,000 m and $f\sim10^{-4}\,\mathrm{s^{-1}}$), and so "the rigid lid" approximation can be adopted. Then, it is possible to define the volume transport stream function ψ such that $-\frac{\partial\psi}{\partial y}=hu$, $\frac{\partial\psi}{\partial x}=hv$. We introduce non-dimensional variables defined as

$$t^*=f_0t \qquad (1)$$

$$(x^*,\ y^*)=L^{-1}(x,\ y) \qquad (2)$$

$$h^*=H^{-1}h \qquad (3)$$

$$\psi^*=(VHL)^{-1}\psi \qquad (4)$$

$$f^*=f_0^{-1}f \qquad (5)$$

V is the characteristic horizontal velocity specified at the inflow opening. We use three different values for V (see Table 1). The notation L is the width of the inflow opening (180 km), and H (150 m) is the depth of the continental shelf. The introduction of ψ and the non-dimensionalization give the the following vorticity equation under the β-plane approximation.

$$\frac{\partial Z}{\partial t}+R_0\left\{\frac{\partial}{\partial x}\left(-\frac{1}{h}\frac{\partial\psi}{\partial y}Z\right)+\frac{\partial}{\partial y}\left(\frac{1}{h}\frac{\partial\psi}{\partial x}Z\right)\right\}+f\left\{\frac{\partial}{\partial x}\left(-\frac{1}{h}\frac{\partial\psi}{\partial y}\right)+\frac{\partial}{\partial y}\left(\frac{1}{h}\frac{\partial\psi}{\partial x}\right)\right\}+\alpha\frac{1}{h}\frac{\partial\psi}{\partial x}=\delta\nabla^2Z \qquad (6)$$

where

$$Z=\frac{\partial}{\partial x}\left(\frac{1}{h}\frac{\partial\psi}{\partial x}\right)+\frac{\partial}{\partial y}\left(\frac{1}{h}\frac{\partial\psi}{\partial y}\right) \qquad (7)$$

For simplicity, asterisks were omitted in the equations above. R_0, α and δ in (6) are the Rossby number V/f_0L, $\beta L/f_0$ and R_0/R_e ($R_e=VL/A_h$ is the Reynolds number), respectively. It is convenient to define the following abbrevations:

NL=non-linear term,

$$R_0\left\{\frac{\partial}{\partial x}\left(-\frac{1}{h}\frac{\partial\psi}{\partial y}Z\right)+\frac{\partial}{\partial y}\left(\frac{1}{h}\frac{\partial\psi}{\partial x}Z\right)\right\} \qquad (8)$$

ST=stretching term,

$$f\left\{\frac{\partial}{\partial x}\left(-\frac{1}{h}\frac{\partial\psi}{\partial y}\right)+\frac{\partial}{\partial y}\left(\frac{1}{h}\frac{\partial\psi}{\partial x}\right)\right\} \qquad (9)$$

$BV=\beta$-term, $\alpha\frac{1}{h}\frac{\partial\psi}{\partial x}$, (10)

DF=diffusion term, $\delta\nabla^2Z$, (11)

TC=time change, $\frac{\partial Z}{\partial t}$. (12)

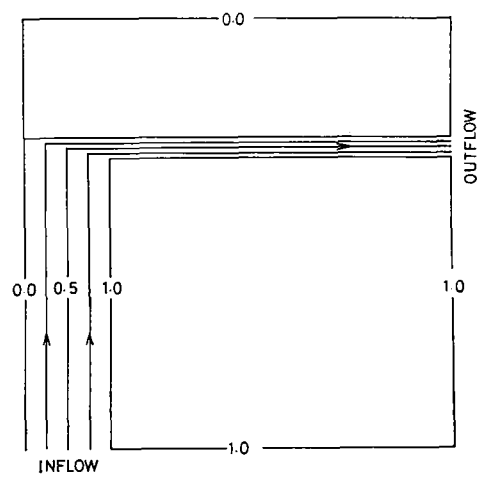

Fig. 2. Initial stream function in a non-dimesional form.

Table 1. Parameters in the four experiments.

Experiment	VHL($\mathrm{cm^3\,s^{-1}}$)	A_h($\mathrm{cm^2\,s^{-1}}$)	R_o	R_e	δ	Integrated time (days)
Case I	2×10^{12}	10^7	4.26×10^{-3}	13.3	3.20×10^{-4}	200
Case II	0.2×10^{12}	10^7	4.26×10^{-4}	1.33	3.20×10^{-4}	200
Case III	2×10^{12}	10^8	4.26×10^{-3}	1.33	3.20×10^{-3}	120
Case IV	20×10^{12}	10^8	4.26×10^{-2}	13.3	3.20×10^{-3}	120

The initial stream function is shown in Fig. 2. The water supplied into the model ocean through the inflow opening flows northward, turns to the right at the latitude of the outflow opening, and flows out through the outflow opening. The values of the volume transport stream functions at the inflow and outflow openings increase and decrease linearly in the x and y-directions, respectively. The values of the volume transport stream function at lateral boundaries and the two openings are fixed during each run of the calculations.

The viscous condition is imposed at the lateral walls:

$$\frac{\partial \psi}{\partial n}=0, \quad \text{at the lateral walls.}$$

And we assume

$$\frac{\partial^2 \psi}{\partial n^2}=0, \quad \text{at the two openings.}$$

The notation $\frac{\partial}{\partial n}$ indicates a local derivative with respect to the coordinate normal to the wall. The dimensional grid intervals are 22.5 km in both directions. This value is small enough to resolve the continental slope. We carried out four experiments (Cases I to IV) as shown in Table 1. The volume transport through the openings and the coefficient of eddy viscosity in Case I are the same as those in the model reported previously by YOON (1982).

3. Results

Figure 3 shows the time change of non-dimensional total kinetic energy $\frac{1}{2}\iint_S h(u^2+v^2)ds$ for Case I, which becomes almost stationary on the 100th day, where S is the surface area of the model ocean. Figure 4 shows the sequential

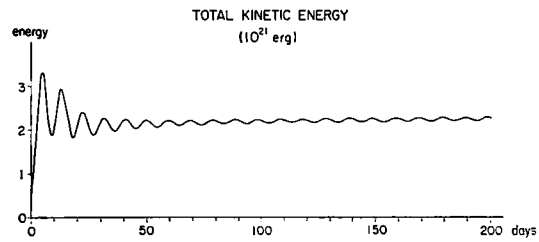

Fig. 3. Non-dimensional total kinetic energy for Case I.

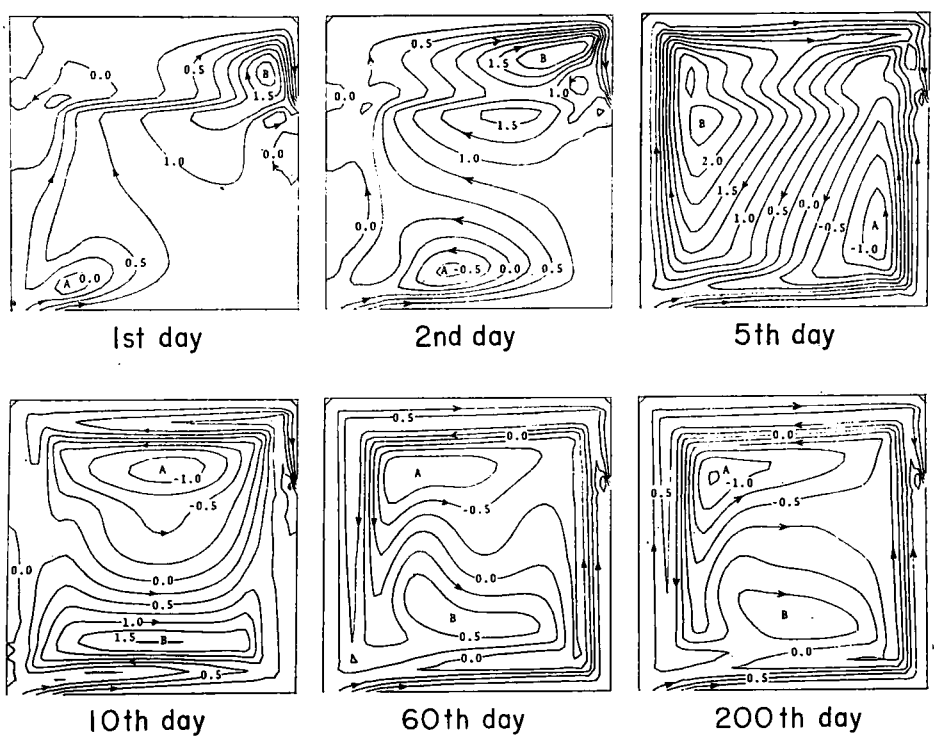

Fig. 4. Sequential patterns of the volume transport stream function in a non-dimensional form for Case I.

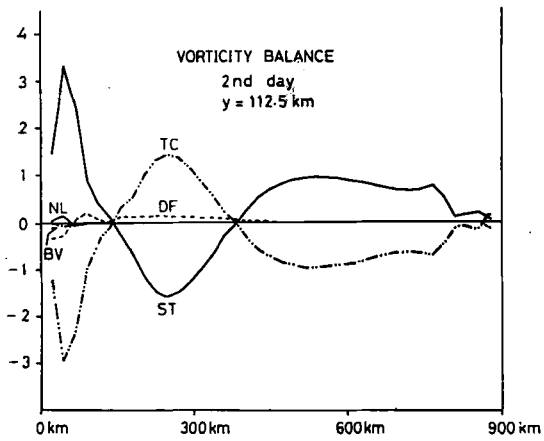

Fig. 5. Vorticity balance along the line of $y=112.5$ km on the 2nd day for Case I.

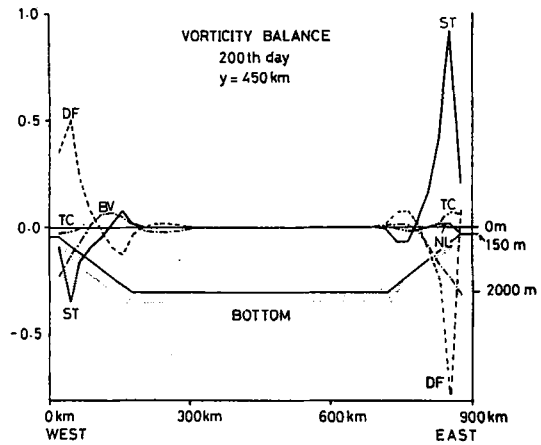

Fig. 6. Vorticity balance along the line of $y=450$ km on the 200th day for Case I.

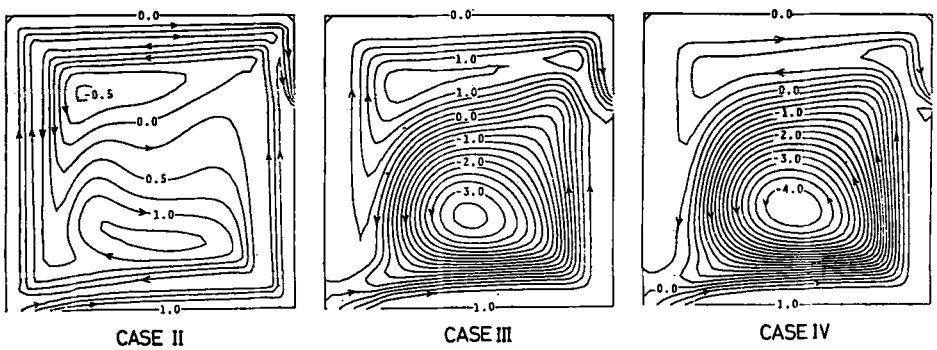

Fig. 7. Patterns of the volume transport stream functions in the steady states for Cases II, III and IV.

patterns of the volume transport stream function for Case I. The initial velocity field induces vortices in the continental slope region due to the stretching and shrinking of the water column. Both the cyclonic vortex, A in Fig. 4 induced by the stretching of the water column near the inflow opening and the anti-cyclonic vortex, B induced by the stretching of the water column near the outflow boundary, propagate along the continental slope with a speed of $2\sim3$ m s^{-1} with the coast to the right until about the tenth day. The speed of propagation of the vortices slows down gradually and the field of the stream function reaches an almost steady state by the 100th day. It should be noted that the stream lines on the continental slope have a tendency to become parallel to the coast during the development of vortices A and B. Figure 5 shows the vorticity balance along the line of $y=112.5$ km on the 2nd day. A good balance holds between the stretching term and the time change of vorticity. This shows that vortices A and B propagate in the continental slope region as continental shelf waves. The lower right figure in Fig. 4 shows the pattern of the stream function on the 200th day. The water supplied into the model ocean basin flows with the coast to the right on the continental slope. A part of it flows out through the outflow opening and the rest of it continues to flow on the outer (seaward) portion of the continental slope. Near the inflow opening, its direction turns to the north, and it flows with the coast to the left on the inner (landward) portion of the continental slope, and flows out through the outflow opening. Figure 6 shows the vorticity balance along the line of $y=450$ km on the 200th day for Case I. On the continental slope

the main balance between ST and DF holds but it is modified by the β-effect.* On the northern and southern continental slope, a good balance between ST and DF holds, though it is not shown in this paper. Figure 7 shows the patterns of the volume transport stream function in almost steady states for Cases II, III and IV. The pattern of the stream function in Case II is similar to that in Case I. As shown in Table 1, the eddy viscosity in Case I is the same as that in Case II, which is one-tenth of that in Cases III and IV. As seen from comparison of the figures in Fig. 4 and Fig. 7, the coefficient of eddy viscosity seems to be an important factor in determining the flow pattern in the model ocean. The volume transport through the openings does not seriously affect the flow pattern within the range under consideration. In all cases, it should be noted that the water supplied into the model ocean, flows with the coast to the right on the continental slope, though the flow pattern in other areas is changeable and depends on the value of eddy viscosity.

4. Discussion

In all cases, most of the water supplied into the model ocean through the southern opening flows along the continental slope with the southern coast to the right. The current along the southern coast (with the width of the continental slope) follow the isobaths of the continental slope except near the inflow opening, where the currents cross the continental slope, maintaining a balance between the stretching and diffusion terms. Continental shelf waves play important roles in the process of adjustment towards a steady state. The currents take the same direction as that of continental shelf waves. Since the density stratification in real oceans does not affect the characteristics of these waves greatly (see YOON, 1974; WANG, 1975), these results are qualitatively applicable to real oceans. As long as the bottom velocity in the Tsushima Strait is significant, part of the water supplied into the Japan Sea will flow along the Japanese coast following the isobaths of the continental slope. According to MIITA (1976), the velocity near the bottom in the Tsushima Strait might be expected to be not so small compared with the velocity at the surface, even in summer. In winter, stratification in the Tsushima Strait is uniform in the vertical direction, and a vertically uniform current structure can be expected. The inclusion of bottom topography as well as the density stratification in numerical models will provide good predictions of the behavior of saline water supplied to the Japan Sea in winter time by reproducing the bottom controlled current obtained here.

Finally it should be noted that the density-driven boundary current obtained in YOON (1982a) might be another component of the nearshore branch of the Tsushima Current, especially in summer.

* If there is not a diffusive effect, it is expected that a balance between ST and BV holds in the eastern and western continental slope regions, and the water would flow along the contour of f/h=constant on the continental slope.

Acknowledgements

The author expresses his hearty thanks to the late Professor Kozo YOSHIDA for his guidance and encouragement during this work.

Thanks are extended to Professors Yutaka NAGATA and Nobuo SUGINOHARA and Dr. Harold SOLOMON for their discussions and careful reading of the manuscript.

References

MIITA, T. (1976): Current characteristics measured with current meters at fixed stations. Bull. Japan Soc. Fish. Oceanogr., (28), 33-58.

WANG, D. P. (1975): Coastal trapped waves in a baroclinic ocean. J. Phys. Oceanogr., **5**, 326-333.

YOON, J. H. (1974): Continental shelf waves in a two-layer ocean. M. S. Thesis. University of Tokyo, 28pp. (in Japanese).

YOON, J. H. (1982): Numerical experiment on the circulation in the Japan Sea. Part I: Formation of the East Korean Warm Current. J. Oceanogr. Soc. Japan, **38**, 43-51.

YOON, J. H. (1982a): Numerical experiment on the circulation in the Japan Sea. Part II: Influence of the seasonal variations of atmospheric conditions on the Tsushima Current in the Japan Sea. J. Oceanogr. Soc. Japan, **38**, 81-94.

日本海の海洋循環についての数値実験
III. 対馬海流の沿岸分枝の力学機構

尹 宗 煥*

要旨: β 面上の2次元順圧モデルを用いて，流入，流出口，そして陸棚および陸棚傾斜をもつ矩形の海で，対馬海流の流路に対する海底地形効果を数値実験により調べた．南の流入口から流れは，定常状態においてはほとんど陸棚と大陸棚斜面上を，岸を右に見て流れ，このような定常状態に遷移する過程において陸棚波が重用な役割を果すことがわかった．このことは，対馬海流の沿岸分枝が，海底地形の制御効果を大きく受けていることを示唆する．

* 東京大学理学部地球物理学教室
文京区弥生2-11-16，〒113